Chapter 6. Photoemission Studies on Zinc Porphyrazine Compounds

6.1 Valence Region

Chapter 5 mainly addressed the problem of fundamental interactions between the ligand and a central metal atom with an incomplete 3d shell in the case of three copper porphyrazine complexes. The size of the ligand, which correlates with the extension of the π-electron system, has proved to influence the charge transfer between the ligand and the central metal. In order to better understand the role of the central metal we also examined the interactions of a metal ion with a fully occupied 3d shell in these porphyrazine molecules. Concerning the central metal ion different processes are expected to take place following the excitation by synchrotron radiation. In this chapter the results for porphyrazine compounds containing zinc as central metal atom will be presented.

Effect of Tert-butyl Substitution on the Photoemission Spectra

The first aspect to be clarified was to estimate the contributions of the tert-butyl groups in the photoemission spectra. For this purpose the photoemission spectra of unsubstituted ZnPc and P1-Zn were measured and compared. In the experimental geometry used in these measurements the synchrotron light impinged onto the sample such that the angle of incidence was 83° and the polarization was 80° with respect to the surface normal. All spectra were obtained in normal emission.

In order to compare the photoemission features of ZnPc and P1-Zn, the corresponding spectra obtained at 98.7 eV excitation energy are displayed in Fig. 6.1-1.

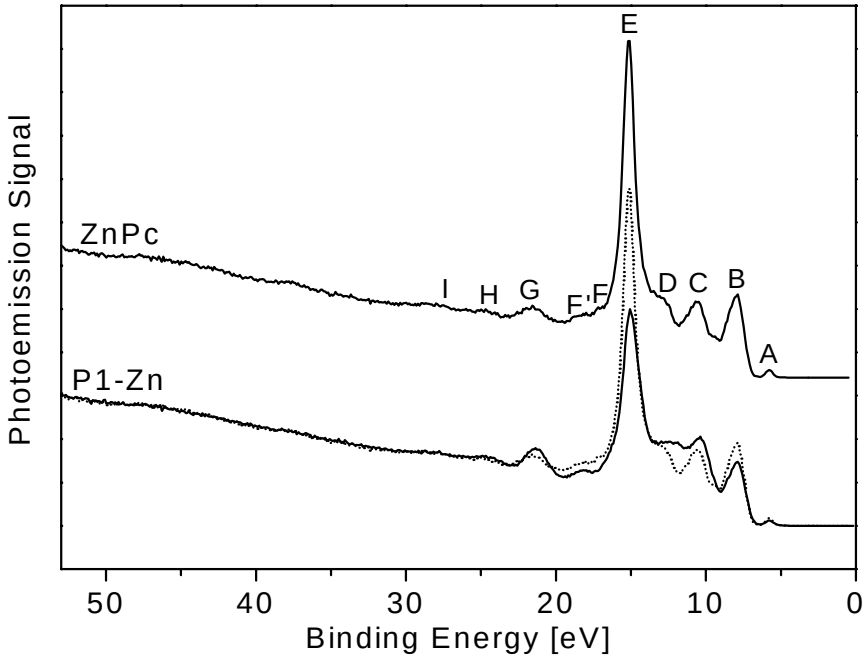

Fig. 6.1-1 Photoemission spectra from standard ZnPc and P1-Zn thin films at 98.7 eV excitation energy (see text for details). The dotted line represents the ZnPc spectrum, plotted on top of the P1-Zn one.

ZnPc (top) and P1-Zn (bottom) spectra are normalized at the background. The spectra are vertically displaced for clarity. In addition, the bottom panel also contains the ZnPc spectrum (dotted) plotted on top of the P1-Zn one. The good background overlap implies that the background shape is not changed by the addition of tert-butyl groups in these Zn compounds.

Only from the direct comparison of ZnPc and P1-Zn spectra, it is difficult to extract the tert-butyl contributions. At first glance the intensities of bands B, E, F and F' seem surprisingly high, they appear larger in the ZnPc spectrum than in the P1-Zn one, even though the latter compound contains additional $C(CH)_3$ groups. As no change of the background shape occurs, the relative intensity of the peaks in the two spectra is attributed to the modification of the Zn/C and N/C ratio for P1-Zn compared to ZnPc and to the fact that the background increases (uniformly) due to the tert-butyl addition. Since the overlap of the two spectra was done at the background, the bands having important Zn (especially band E) or N (band B) contributions appear with lower intensity in the P1-Zn spectrum relative to the corresponding ones in the ZnPc spectrum.

The direct comparison between ZnPc and P1-Zn spectra reveals an increased signal of band G and an increase in the 9.5-13.5 eV binding energy region at the tert-butyl

addition. However, taking into account the comparison between H_2Pc and P1-H_2 spectra and that between CuPc and P1-Cu, it becomes clear that, in fact, tert-butyl contributions are also found in the 13.5-16 eV binding energy region. Probably, the latter contributions are not distinguished in the P1-Zn case since significant Zn signal is found at the same position as well.

Most of the peak positions are rather identical in ZnPc and P1-Zn. Similar to the Cu case, band G is shifted by about 0.2 eV towards lower binding energies and features F' and C are also shifted by the same amount. Bands F and D are not resolved anymore at tert-butyl substitution, a broad signal being found between peaks D and C.

Except for the lower intensity of bands B, E, F and F' in P1-Zn relative to ZnPc, a good overall concordance exists between the changes in the ZnPc spectrum upon tert-butyl substitution and the modifications appearing in H_2Pc or CuPc spectra upon tert-butyl substitution.

Note that the origin of bands E and F is different from those having the identical notations for metal-free compounds. This is because in the case of the Zn complexes, bands E and F include, in addition, Zn contributions.

Metal Features in the Spectra and Assignment of the Peaks

Theoretical calculations using D_{4h} symmetry for ZnPc showed that the HOMO is an a_{1u} orbital which has the same composition (C2p atomic orbitals) as the HOMO for H_2Pc and which is an exclusive ligand orbital with π character [NgP2001, LiS2001, CWZ2001, SHG2001]. In a different study 2% contribution from pyrrole nitrogens, additional to the C2p character, has been claimed [RRB2001]. The HOMO-1 is calculated to be a b_{1g} orbital with relatively low Zn $d_{x^2-y^2}$ contribution (given as 12% in [RRB2001] and 20% in [LiS2001]) but with significant pyrrole nitrogen lone pairs and carbon character [RRB2001]. A large energy separation (~1.1 eV) is found between the HOMO-1 and the HOMO. The HOMO-2 orbital mainly arises from the meso-bridging nitrogen atoms but also from the pyrrole nitrogens and carbons [RRB2001]. The very next occupied orbitals are calculated to have mainly mixed contributions from carbon and nitrogen atomic orbitals. The Zn3d shell is almost unperturbed in the low energy part of the electronic spectrum. The only Zn3d orbital which interacts to a certain degree with the macrocycle is $d_{x^2-y^2}$ [RRB2001]. With the exception of the HOMO-1, the occupied molecular orbitals which include Zn3d contributions are found in an energy interval separated by (7.96-8.94) eV from the HOMO energy [RRB2001].

In the case of Zn-tetraazaporphyrin the HOMO is calculated to derive from the same type of atomic orbitals as in ZnPc, being an a_{1u} orbital as well. It is also found to be well separated from the HOMO-1 [NgP2001].

In ZnPc, although the metal atom has a formal charge of +2, the charge distribution is calculated to be $3d^{10}4s^{0.55}4p^{0.81}$ [LiS2001]. Similar to the case of other metal phthalocyanines, the fact that there is charge on 4s and 4p suggests that the bonding between metal (Zn) and Pc is not purely ionic but significantly covalent [LiS2001].

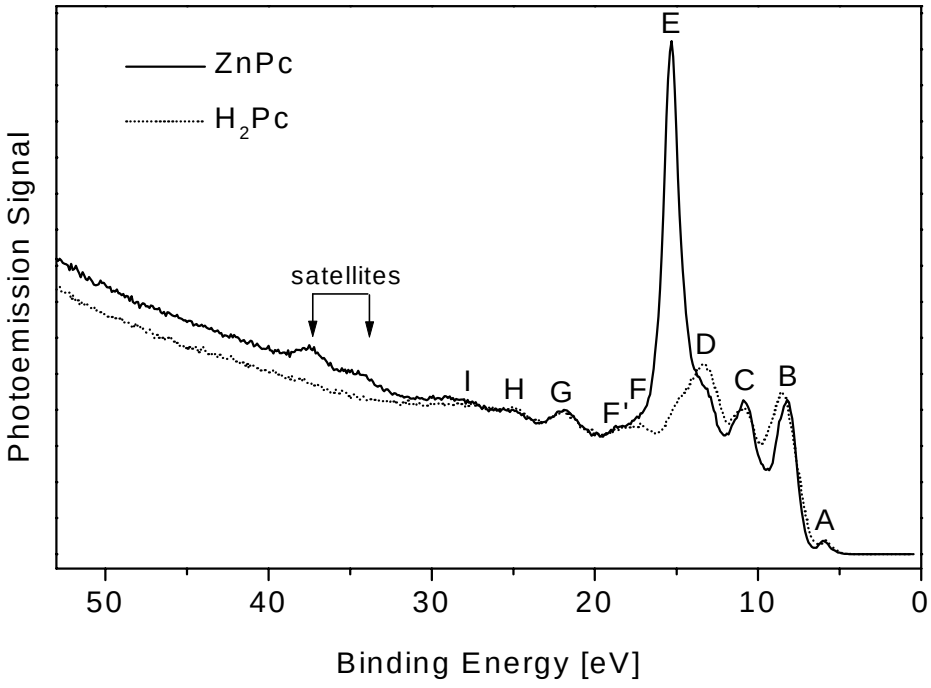

Fig. 6.1-2 Photoemission spectra from unsubstituted ZnPc and H_2Pc. The main zinc contributions in the spectra are evidenced. They are the Zn3d direct emission line (at the position of band E) and Zn satellite peaks (as labeled).

In order to identify the zinc contributions and to emphasize the photoemission spectral changes induced by the replacement of the two central hydrogen atoms by a zinc one, the spectra of zinc complexes have been compared with those of the respective metal-free compounds. The spectra of ZnPc and H_2Pc are displayed in Fig. 6.1-2. For the same purpose, the photoemission spectra of P0-Zn, P1-Zn, and P2-Zn are represented in Fig. 6.1-3 together with the experimental data for their corresponding metal-free compounds. All these data have been measured at 89.6 eV under identical experimental conditions.

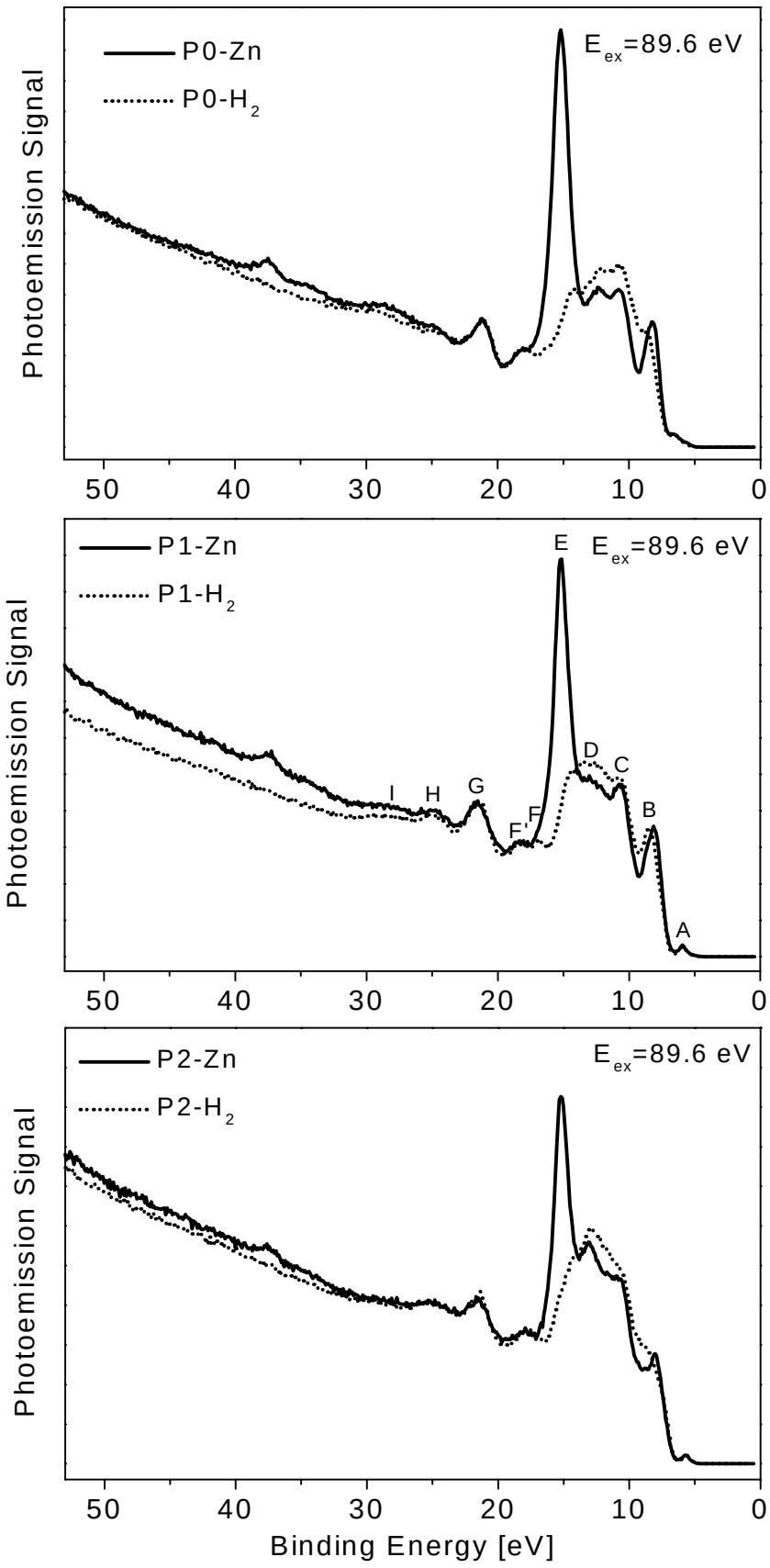

Fig. 6.1-3 Photoemission spectra of P0-Zn, P1-Zn and P2-Zn in comparison with the spectra of the respective metal-free compounds. Photon energy was 89.6 eV for all spectra.

The spectrum of P3-Zn is not included since this film could not be prepared by UHV sublimation, and the film obtained by the wet chemical method is unstable. The spectra have been normalized in order to achieve an optimum overlap in the region of ligand feature G. The reason for having certain ligand features in Fig. 6.1-2 and Fig. 6.1-3 appearing with higher intensity for the metal-free compounds than for the Zn ones is similar to that invoked in the case of Cu complexes. Relative to a pure ligand peak the background signal is larger in the photoemission spectra of a zinc porphyrazine than in the spectra of its corresponding metal-free compound. As the signal in the region where the normalization is done is influenced by the background intensity, in Fig. 6.1-2 and Fig. 6.1-3 certain ligand features show less intensity for the zinc compounds than for the analogous metal-free ones.

By comparing the spectra of Zn- and metal-free compounds in the two figures mentioned above, one notices that the shape of the background is also affected to some degree by the presence of the zinc atom in the compounds (e.g. the background slope is different for P1-Zn and P1-H_2). The effect depends on the type of the molecule.

In view of the above mentioned theoretical results, and accounting for the fact that P0-Zn, P1-Zn and P2-Zn are chemically very similar to Zn-tetraazaporphyrin, ZnPc and Zn-naphthalocyanine, respectively (see pag. 2), it appears that band A in the P0-Zn, P1-Zn and P2-Zn spectra (Fig. 6.1-2 and Fig. 6.1-3) originates from the HOMO of the molecules. According to theory, band B includes, additionally to nitrogen and carbon contributions (like for the metal-free compounds), also a Zn signal, though to a small amount [LiS2001, RRB2001]. The features C, D, F', G, H, and I in the spectra of zinc compounds seem to have a one-to-one correspondence to those of the analogous metal-free complexes. This indicates that these features contain the same contributions as the respective bands in the metal-free compounds. Compared to the metal-free compounds, band B is found at lower binding energy (~0.3 eV), band D has a 0.2 eV higher binding energy for P0-Zn and P2-Zn, while all the other ligand features are found at identical positions.

In Fig. 6.1-2 and Fig. 6.1-3 at approximately 37.5 and 34.2 eV binding energy, one notices two peaks which are not visible in the spectra of the metal-free compounds and also not clearly distinguishable in the spectra of ZnPc nor P1-Zn at 98.7 eV (Fig. 6.1-1). Those features correspond to the Zn satellite signal [IKCH80] and are well visible in the spectra only if the 3p-4s excitation in the central Zn^{2+} takes place. The origin of the satellite peaks and their properties will be discussed in detail in section 6.4.

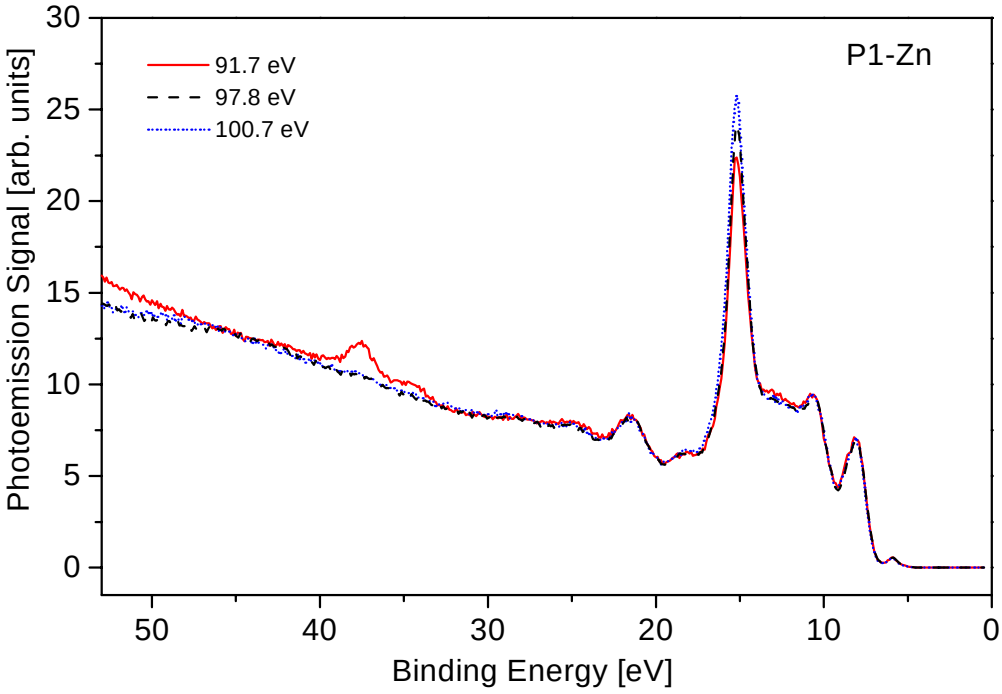

Fig. 6.1-4 Photoemission spectra of P1-Zn for different excitation energies evidencing the intensity increase of band E (which includes Zn3d direct photoemission signal) relative to the ligand peaks for increasing photon energy.

In Fig. 6.1-4 background normalized photoemission spectra of the P1-Zn compound for photon energies of 91.7, 97.8, and 100.7 eV are shown. Increasing the excitation energy has little effect on the relative spectral intensities, except for the enhancement of band E relative to the ligand features and a change in the satellite signal (which will be discussed in section 6.4). The intensity changes of band E correlate with the cross section variations due to its Zn3d character. Specifically, the cross section ratios between Zn3d and C2s and between Zn3d and C2p increase for increasing photon energy in this energy range [Yeh93]. No intensity changes are observed for band B as a function of photon energy. The interpretation that follows is that the Zn3d character of this feature is very low. As previously mentioned, at most 20% of the HOMO-1 is calculated to have Zn3d character but one should consider that feature B includes also contributions from other orbitals which are exclusively derived from carbon and nitrogen.

Evolution of the Photoemission Features as a Function of Ligand Size

In order to underline the changes of the photoemission features for increasing ligand size, the spectra of P0-Zn, P1-Zn, and P2-Zn obtained for 91.7 eV photon energy

are plotted in Fig. 6.1-5. All spectra have been normalized to unity at the maximum of the Zn3d band and were then vertically translated for clarity.

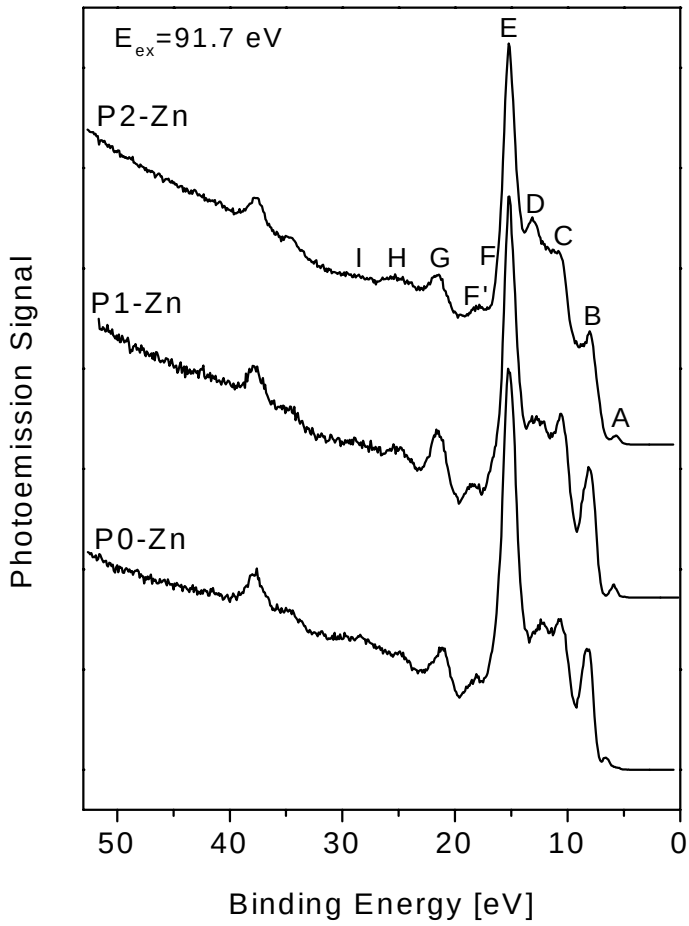

Fig. 6.1-5 Photoemission spectra of P0-Zn, P1-Zn, and P2-Zn at 91.7 eV excitation energy. Notice the intensity increase of the benzene features relative to the Zn ones with the increase of the ligand size.

One notices a growing of the features arising from the aromatic units in the molecule and of the background relative to the Zn3d peak as the ligand size is extended.

The position of the Zn3d main line is identical for all these Zn compounds, being located at 15.2±0.07 eV binding energy. This is expected considering that this peak mainly contains contributions from zinc, from carbon and nitrogen atoms in the central ring, and from tert-butyl. Also the Zn satellite peaks appear at the same binding energy for P0-Zn, P1-Zn and P2-Zn. No shift is observed for band C, which is quite different as compared to the case of metal-free compounds. Moreover, band I shows constant position in the spectra.

The changes in the positions of bands H and G with increasing ligand size are consistent with those observed for copper- and metal-free compounds. They have constant

binding energy in the benzene containing complexes (P1-Zn and P2-Zn) and shift towards lower values by 0.2 and 0.6 eV, respectively, for P0-Zn. A shift of about 0.35 eV towards lower binding energies is also observed for feature F' in P2-Zn as compared to its position in P0-Zn and P1-Zn spectra.

A blow-up of the edge of the valence region is presented in Fig. 6.1-6. As for the case of the metal-free and the copper compounds, a binding energy decrease of feature A (derived from HOMO) with the enlargement of the ligand is observed. The HOMO binding energies are determined to be 6.63±0.07, 5.97±0.07, and 5.69±0.07 eV for P0-Zn, P1-Zn and P2-Zn, respectively. In these zinc compounds feature A is derived from the HOMO of the molecules and the HOMO has the same composition as for the corresponding metal-free compounds. Thus, for the two classes of compounds the HOMO destabilization upon linear benzoannelation results from the same cause.

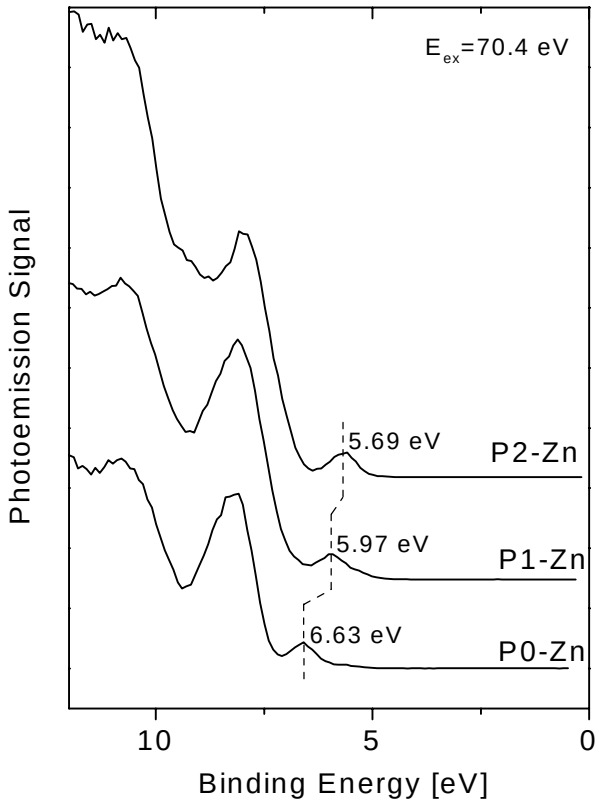

Fig. 6.1-6 Photoemission spectra for P0-Zn, P1-Zn, and P2-Zn at the edge of the valence region. All spectra were obtained for 70.4 eV photon energy. The binding energy of feature A decreases when the ligand gets larger. The labels mark the respective binding energies. All values are given with ±0.07 eV uncertainty.

As shown in [OCP96], the HOMO is mainly localized on the central porphyrazine ring and the antibonding interactions with the fused benzo-units at linear benzoannelation determine a decrease of its binding energy. Since the effect is weaker for the outer benzene units as compared to the inner ones, the difference in HOMO binding energy between P2-Zn and P1-Zn is smaller than the one between P1-Zn and P0-Zn.

It is further noticed that the HOMO binding energies are determined to be slightly larger (by 0.05-0.08 eV) for the zinc compounds than for the similar metal-free ones. However, the relative differences in the HOMO binding energy between two compounds in the Zn series are nearly the same as between the corresponding complexes in the metal-free series (they differ by 0.01-0.02 eV).

Additionally, one observes that band B shifts slightly at the extension of the ligand, yielding a binding energy of 8.2±0.07, 8.1±0.07, and 8.00±0.07 eV for P0-Zn, P1-Zn and P2-Zn, respectively. This possibly reflects the effect of benzene contributions which gradually increase at the enlargement of the ligand. A similar effect was also observed in the case of metal-free compounds.

Note that in all spectra from Fig. 6.1-5 and Fig. 6.1-6, the Zn3d main line is found at an identical binding energy, 15.2±0.07 eV.

6.2 Photodegradation Effects

In order to examine the photostability of these zinc materials, their photoemission spectra were measured for different synchrotron radiation exposure times. Identification of spectral changes is important for judging the quality of the measured data and for determining the degree and the manner in which the features of main interest (as for example the satellite features or the peak originating from the HOMO) are changed as a result of synchrotron light exposure.

Fig. 6.2-1 presents the photoemission spectra of P0-Zn obtained from an identical spot but for two synchrotron radiation exposure times.

Band A is one of the strongly changing features in the P0-Zn photoemission spectrum, due to photodegradation. It smears out and broadens so that for long exposures the top of the peak cannot be distinguished anymore. Features B, C, D, F’ and G broaden and smear out as well but their changes appear for longer exposure times as compared to the case of band A. From the spectra of P0-Zn obtained for 91.7 eV photon energy, it is inferred that the Zn satellite peaks are not significantly affected by irradiation.

Comparing the photodegradation effect for P0-Zn with the one observed after the same synchrotron radiation exposure time for P0-H_2, it appears that the P0-Zn sample is less affected by irradiation. As the photon flux was similar in both measurements, this suggests that the presence of the central zinc atom stabilizes the molecule with respect to photodegradation.

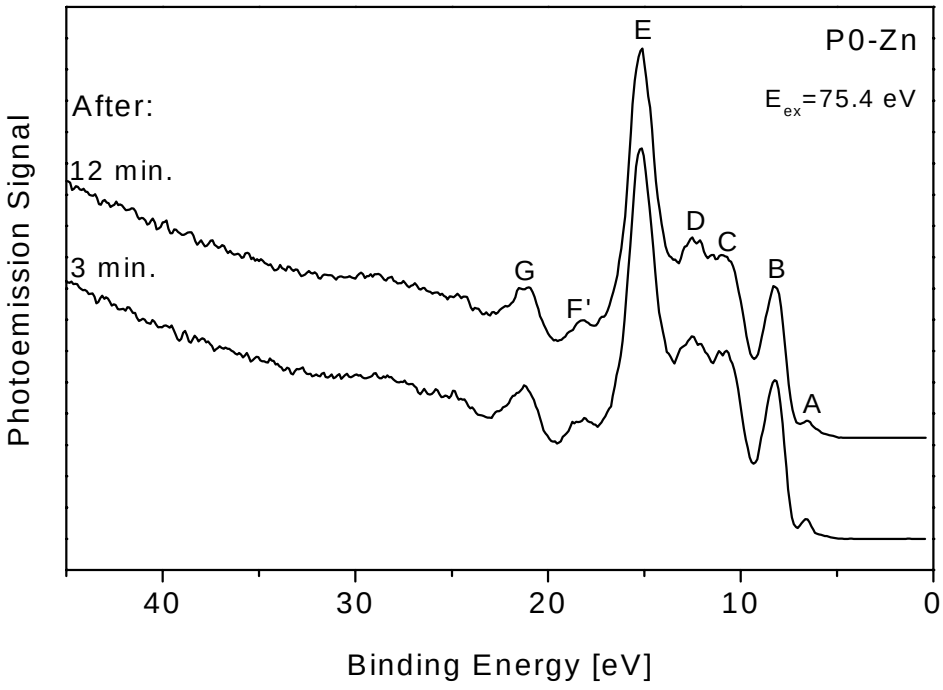

Fig. 6.2-1 Photoemission spectra of P0-Zn for different synchrotron radiation exposure times. The spectra were measured at 75.4 eV photon energy. They were normalized at the background and then vertically translated for clarity. Band A (derived from HOMO) is one of the features in the spectrum changing strongly as a result of photodegradation.

In order to show the changes induced by the synchrotron radiation exposure in the P1-Zn spectrum, the photoemission spectra of the P1-Zn film obtained for two irradiation times are displayed in Fig. 6.2-2. The spectra were measured using 91.7 eV photon energy. They have been normalized in order to obtain an optimum background overlap. The exposure time difference between the two spectra has been chosen to be sufficiently large, in order to clearly observe the modifications of the photoemission features. The changes of the P1-Zn spectrum appear for larger irradiation times as compared to P0-Zn. In Fig. 6.2-2 one observes that for P1-Zn the bands A, B, C, D, F' and G are affected by

photodegradation. These features become broader and smeared out in time. Band E shows only a slight broadening, while the satellite peaks are nearly unaffected.

Similar investigations performed for P2-Zn showed that this is the most stable compound in this series with respect to synchrotron radiation exposure (similarly to its corresponding metal-free and copper complexes). The changes of the photoemission features caused by beam exposure resemble those previously described for P1-Zn.

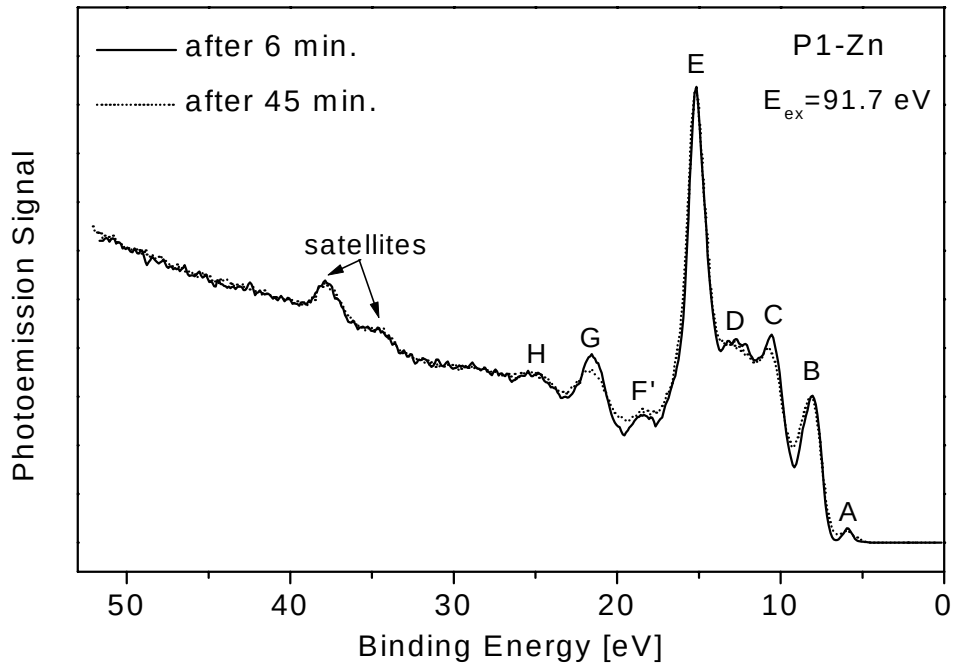

Fig. 6.2-2 Photoemission spectra of P1-Zn for different synchrotron radiation exposure times. The changes of the photoemission features induced by the synchrotron radiation exposure can be traced.

In conclusion, the photoemission spectral changes of zinc complexes due to photodegradation correlate with those observed for the respective metal-free and copper compounds. Within the zinc complexes, P0-Zn seems to be the most sensitive compound with respect to synchrotron radiation exposure. Thus, the central porphyrazine ring is most strongly affected by photodegradation, and consequently also the peak derived from the HOMO of molecules. The satellite peaks seem rather unaffected by synchrotron exposure. However, irrespective of the different photosensitivity, measurements were always performed by frequently changing the exposed sample spot.

6.3 XPS Measurements

In order to give a more comprehensive characterization of the Zn series of molecules, in addition to the UPS/VUV investigations, XPS measurements were performed. Main focus in the present XPS studies was on the analysis of N1s and Zn2p core levels regions since these are particularly sensitive to changes in the Zn-N bonding character.

Data obtained for UHV-sublimed P0-Zn, P1-Zn and P2-Zn films will be presented in the following. For excitation, non-monochromatized Al Kα radiation (main excitation energy hν=1486.7 eV) was used. For every compound the binding energy scale was determined with reference to the carbon C1s peak centered at 284.2 eV. It is to be noticed that for all these zinc compounds the C1s peak contains the respective signal from the carbon atoms found in the inner porphyrazine ring, in the benzene units, and four tert-butyl groups. The only number of carbon species that changes is the one from benzene moieties.

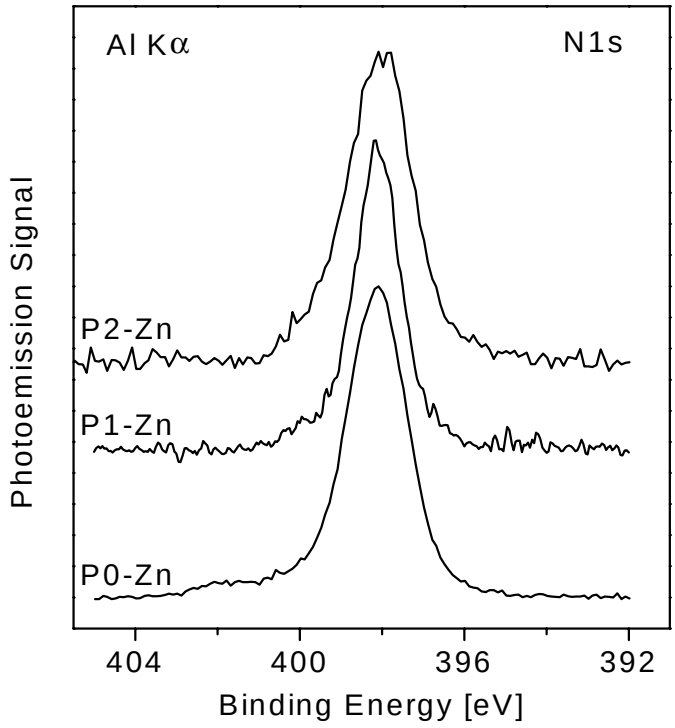

Fig. 6.3-1 N1s core level in the XPS spectra of P0-Zn, P1-Zn and P2-Zn

The N1s and C1s spectra of the P0-Zn, P1-Zn and P2-Zn compounds are plotted in Fig. 6.3-1 and Fig. 6.3-2. A Shirley type background has been subtracted from these spectra.

In Fig. 6.3-1 the N peaks have been vertically translated for clarity. For each molecule, the N1s peak contains the contributions of meso-bridging and pyrrole nitrogens and also a satellite (on the high binding energy side) originating from a $\pi \rightarrow \pi^*$ valence excitation associated with the core ionization of the pyrrole nitrogens [CRD92, OLR99]. As seen in Fig. 6.3-1, the N1s peak is found at 398.1±0.2 eV for P0-Zn and P1-Zn and 398±0.2 eV for P2-Zn.

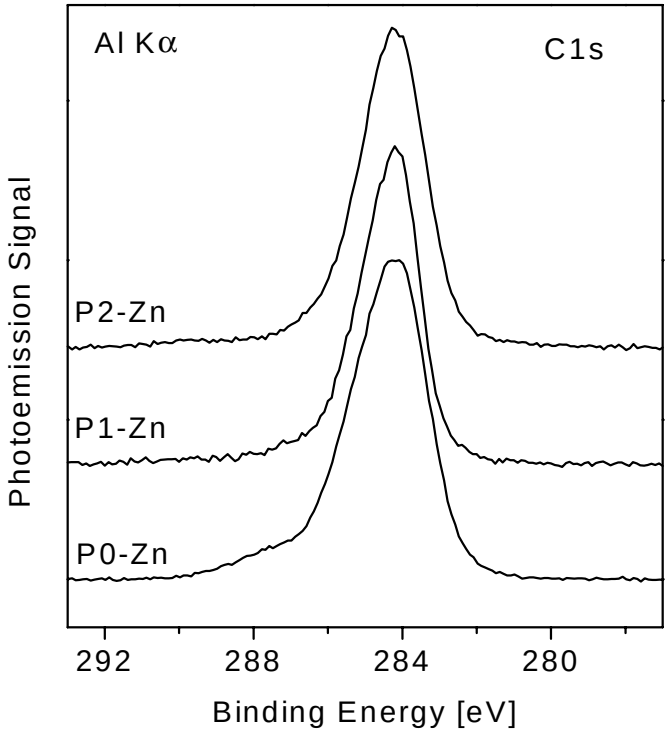

Fig. 6.3-2 C1s core level in the XPS spectra of P0-Zn, P1-Zn and P2-Zn

In Fig. 6.3-2 the C1s spectra have been normalized to the peak height and then vertically translated. The C peaks have an asymmetric lineshape with a longer tail on the high binding energy side. Studies on unsubstituted phthalocyanines and naphthalocyanines have shown three types of contributions giving rise to the C1s peak: the contribution of the aromatic carbons (which is the main contribution for unsubstituted phthalocyanines and naphthalocyanines), that of the pyrrolic carbon atoms (found at 1.4 eV higher binding energy than the aromatic carbons in benzene) and a shake-up satellite (located on the high

binding energy side) [ONL97, OLS97, OLS99]. The satellite, which is at an approximately 1.6-2.0 eV higher binding energy as compared to the pyrrole carbon peak, has been attributed to a π-π* satellite excitation of the latter [NKT74, ONL97].

In the present case, for P0-Zn, P1-Zn and P2-Zn, in addition to the above-mentioned contributions, the XPS signal of carbon atoms from tert-butyl is added. From the present low-resolution XPS measurements, it is difficult to distinguish the contributions originating from the different types of carbon atoms. To our knowledge no other XPS studies on tert-butyl containing porphyrazines were performed up to date.[1]

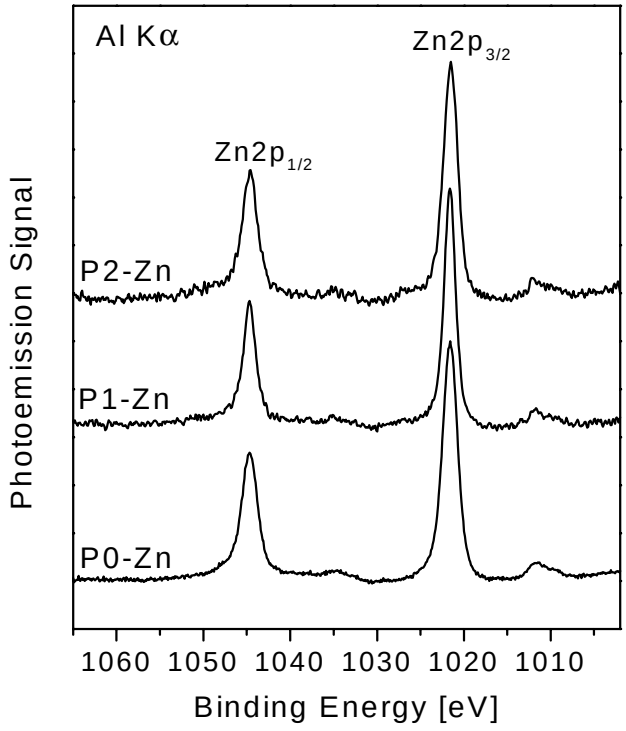

Fig. 6.3-3 Zn2p core level region of the XPS spectra of P0-Zn, P1-Zn and P2-Zn. No shift is detected for the two spin-orbit split components, $Zn2p_{1/2}$ and $Zn2p_{3/2}$, at the enlargement of the ligand.

Spectra depicting the near Zn2p core levels region are presented in Fig. 6.3-3. A linear background has been subtracted from these XPS spectra. The curves have been

[1]The smaller widths of C1s and N1s peaks for the P1-Zn compound in Fig. 6.3-1 and Fig. 6.3-2 are interpreted to be caused by the different pass energy used during these measurements (E_p=10 eV). For the other two zinc compounds the pass energy was E_p=20 eV.

normalized to the $Zn2p_{3/2}$ peak height. For P0-Zn and P1-Zn, the $Zn2p_{3/2}$ and $Zn2p_{1/2}$ binding energies are determined to be 1021.6±0.2 eV and 1044.7±0.2 eV, respectively. For P2-Zn, the $Zn2p_{3/2}$ and $Zn2p_{1/2}$ peaks are found at 1021.5±0.2 eV and 1044.6±0.2 eV, correspondingly. The absence of appreciable satellite features in the XPS spectra of ZnPc and other Zn porphyrins has been reported previously [MuH79]. In the present spectra the small peaks observed at about 10 eV lower binding energy than the $Zn2p_{3/2}$ and $Zn2p_{1/2}$ peaks are due to the excitation of the sample by the less intense $AlK\alpha_{3,4}$ radiation components.

6.4 Satellite Peaks in the Spectra of the Valence Region for Zinc Porphyrazines

As the photon energy is increased from 86 to 101 eV, one notices the developing and subsequent decrease of two satellite peaks located at approximately 34.7 and 37.8 eV binding energy. For the excitation energies used in the experiment, the intensity maximum of these peaks is at 91.7 eV. The photoemission spectra of P0-Zn, P1-Zn and P2-Zn obtained for 91.7 and 87.1 eV excitation energy are displayed in Fig. 6.4-1. One can see that the satellite features are hardly distinguishable for 87.1 eV photon energy while they are clearly observable for 91.7 eV photon energy. At the increase of the ligand size, no shift was observed for these satellite peaks.

Fig. 6.4-2 presents photoemission spectra (smoothed by adjacent average) of ZnPc, P0-Zn, P1-Zn and P2-Zn thin films in the region of the satellite peaks for the photon energies used in these measurements. The spectra have been normalized at the signal for 30 eV binding energy and were then vertically translated for clarity. This presentation allows to directly trace the evolution of the peak intensity of the satellite as a function of the excitation energy. It also reveals a discontinuity that exists between the ZnPc spectra for 93.2 and 93.7 eV photon energy, which most probably arises from inhomogeneous ZnPc film patches. No systematic binding energy shift of the satellite peaks is observed as a function of photon energy.

A blow-up of the zinc satellite region for ZnPc and P1-Zn spectra measured at 86.6, 91.7 and 101.2 eV is displayed in Fig. 6.4-3. In the case of ZnPc the spectrum for 85.6 eV excitation energy is also added. As opposed to the copper case, the Zn satellite features are not well distinguished throughout the entire excitation range.

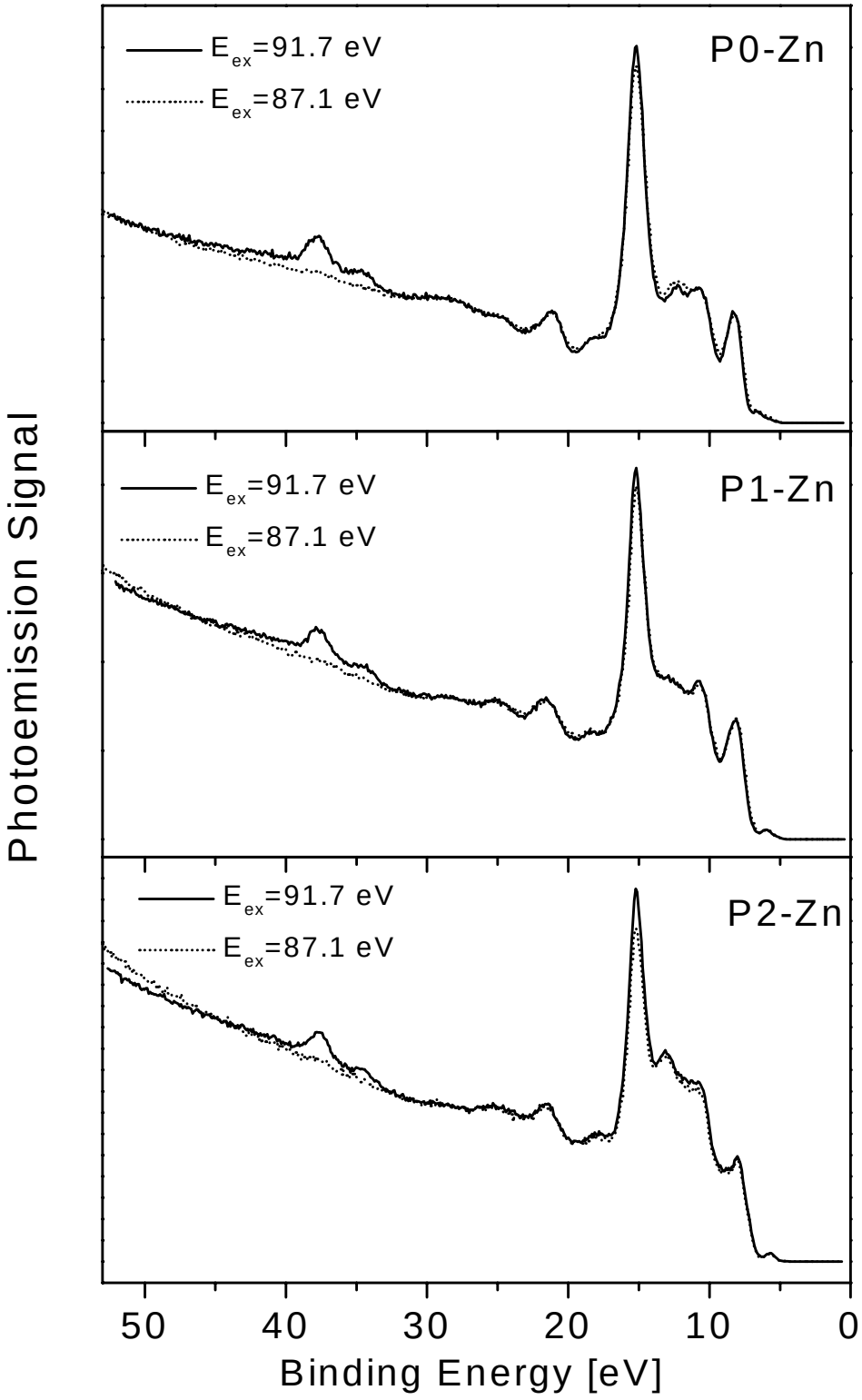

Fig. 6.4-1 Photoemission spectra of P0-Zn, P1-Zn, and P2-Zn for 91.7 eV (solid line) and 87.1 eV (dotted line) photon energy.

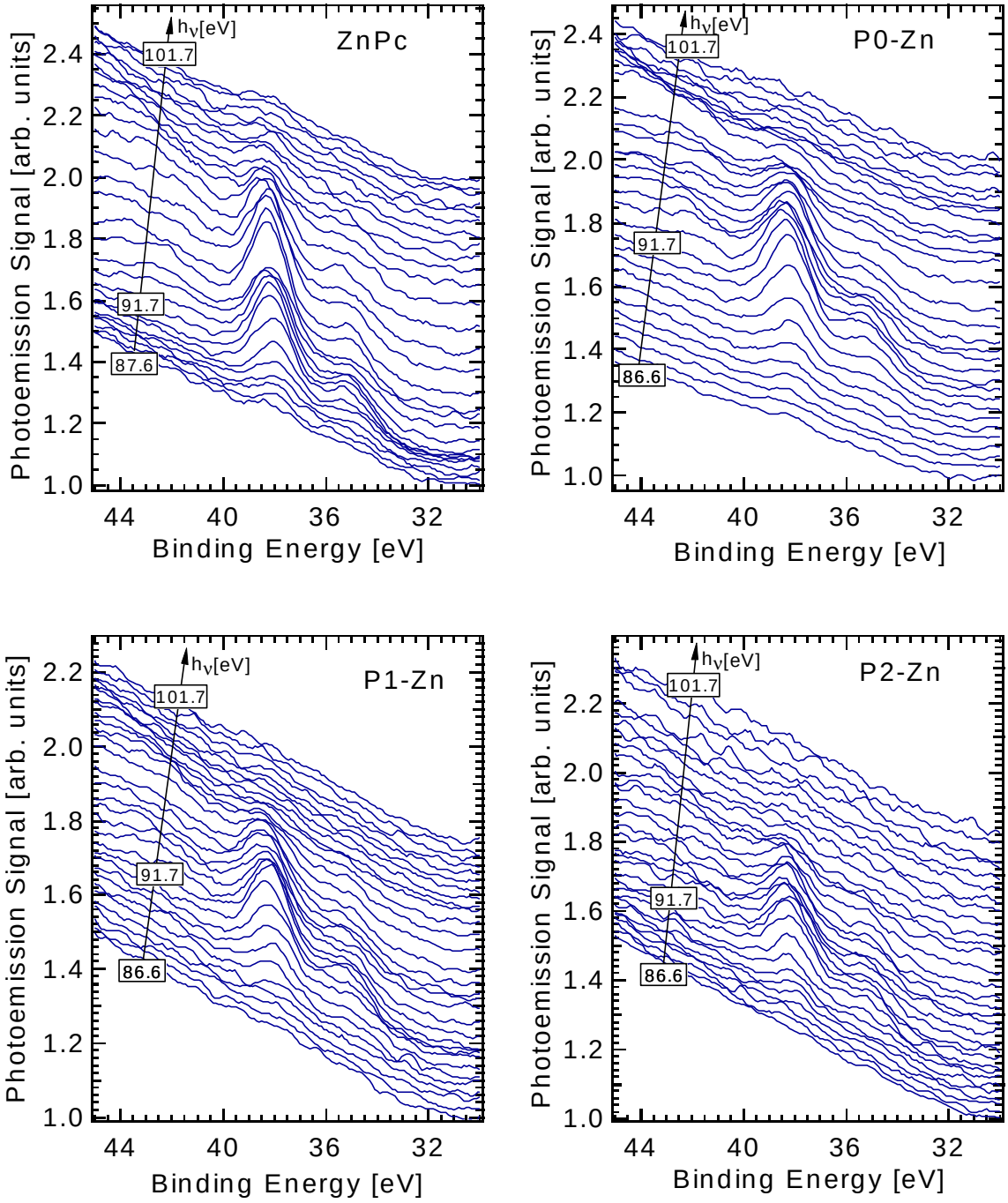

Fig. 6.4-2 Photoemission spectra (smoothed) in the region of Zn satellite peaks for ZnPc, P0-Zn, P1-Zn and P2-Zn for the photon energies used in the present experiments (from bottom to top: 86.6, 87.1, 87.6, 88.1, 88.6, 89.1, 89.6, 90.1, 90.6, 91.1, 91.7, 92.2, 92.7, 93.2, 93.7, 94.2, 94.7, 95.1, 95.7, 96.2, 96.8, 97.2, 97.8, 98.2, 98.7, 99.2, 99.8, 100.2, 100.7, 101.2, 101.7 eV). The graph for P0-Zn is missing the 100.7 eV photon energy curve, and the ZnPc graph is missing the spectra for 86.6 and 87.1 eV photon energy. One can note the evolution of the satellite peaks intensity at the variation of photon energy.

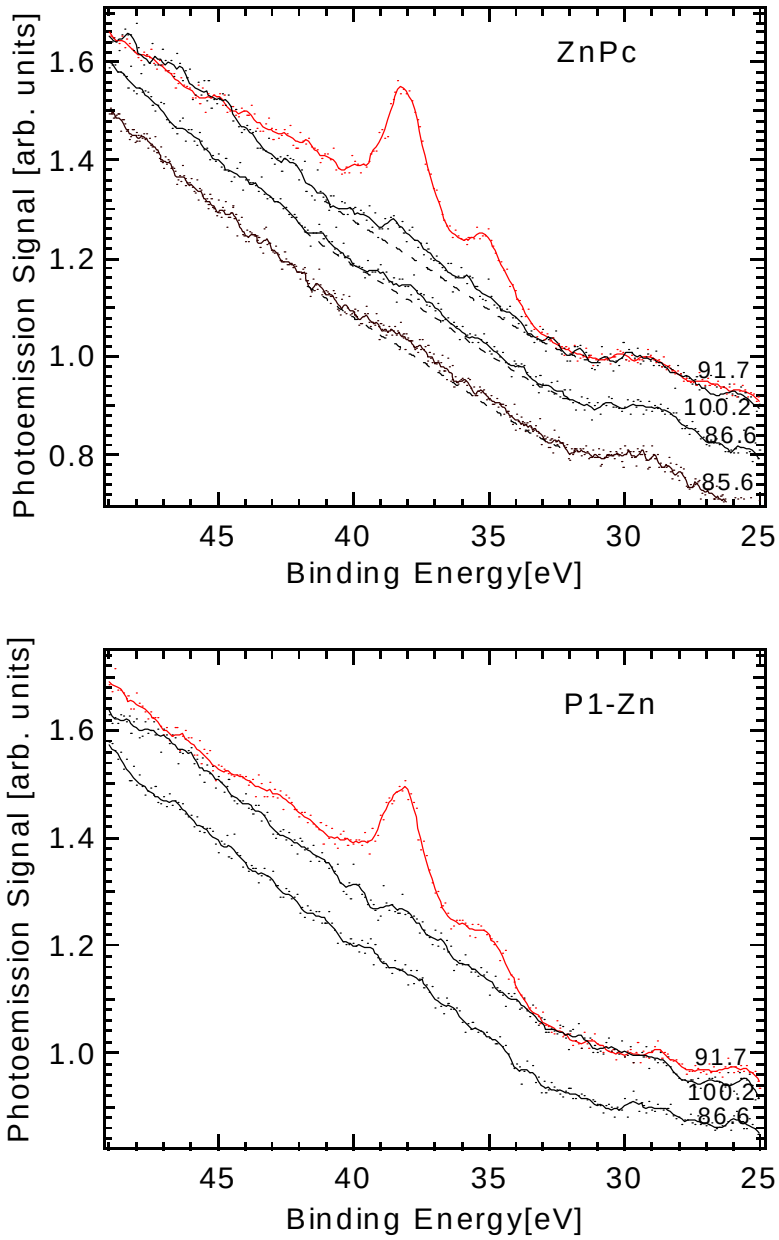

Fig. 6.4-3 Photoemission spectra of ZnPc and P1-Zn in the region of Zn satellite peaks obtained for 86.6, 91.7 and 100.2 eV photon energy. For ZnPc the spectrum at 85.6 eV is also shown. One can note that a weak satellite signal is visible in the ZnPc spectra, even for 85.6, 86.6, and 100.2 eV photon energy. The dashed line in the upper graph serves to guide the eye.

In Fig. 6.4-3 one can note that for ZnPc a weak signal is still perceptible at the position of the Zn satellite peaks for 85.6, 86.6 and 100.7 eV photon energies while such a signal is not distinguishable for P1-Zn nor P0-Zn or P2-Zn. However one has to consider that a weak Zn satellite signal for these excitation energies is also present in the photoemission curves of P0-Zn, P1-Zn and P2-Zn, but is masked by the larger background as compared to the ZnPc case. The excitation energy region for which these zinc satellite

peaks may be well distinguishable depends to some extent on the background signal. A reduced background signal (like in ZnPc) favors the good observance of the satellite signal in a slightly larger photon energy interval (Fig. 6.4-2 and Fig. 6.4-3).

It is generally accepted that in ZnPc the zinc is divalent (see for example [RRB2001, LiS2001]), hence the 4s level is formally unoccupied. Considering the similar chemical structure and behavior of P0-Zn, P1-Zn and P2-Zn on one side and the similarity between P1-Zn and ZnPc on the other side, it follows that the central zinc is also divalent in these porphyrazine compounds.

This kind of zinc satellite peaks were previously observed for ZnPc [IKC80] and ZnO [DCB88]. They result from a 3d ionization process with shake-up, which leads to a $3d^8 4s^1$ final-state configuration of zinc (two holes in the Zn3d subshell and one electron in the 4s level) [ITK86]:

$$3p^6 3d^{10} 4s^0 + h\nu \rightarrow 3p^6 (3d^8 4s^1) + e^-.$$

The enhancement of the satellite peaks observed for certain photon energies was interpreted as the result of a 3p-4s excitation accompanied by an Auger decay of a 3d electron with the emission of another electron from the 3d level. For the particular case of ZnPc this interpretation was previously emerging in the hypothesis that the central zinc can be treated as quasitatomic in ZnPc and due to the s-p hybridization there would be empty 4s states which, in the presence of a core hole, are localized [IKC80]. The existence of two satellite peaks was attributed to $3d^8$ multiplets [IKC80]. Consequently, we conclude that the process giving rise to the enhancement of the Zn satellite peaks is the 3p-4s excitation accompanied by a 3d Auger decay, but noting that the holes in the Zn4s level exist mainly due to the fact that the central zinc has a formal Zn^{2+} oxidation state in these compounds. In a simple model, this process can schematically be described as

$$3p^6 3d^{10} 4s^0 + h\nu \rightarrow 3p^5 3d^{10} 4s^1 \leftrightarrow 3p^6 3d^8 4s^1 + \text{Auger electron},$$

hence the obtained final state is again $3d^8 4s^1$ [IKC80]. The same final state of the system is thus reached by ionization with shake-up and as result of the 3p-4s excitation. Consequently, the coherent superposition of the Auger electron and the electron resulting from photoionization with shake-up takes place, which leads to the enhancement of the satellite peaks. These respective processes are sketched in Fig. 6.4-4.

In addition to the satellite features, above the threshold energy $M_{2,3}M_{4,5}M_{4,5}$ Auger peaks appear [IKC80]. In the present series of spectra they are observed on the high binding energy side of the satellites for excitation energies larger or equal to 91.7 eV (see Fig. 6.4-5 and also Fig. 6.4-2, Fig. 6.4-3). The Auger signal is broad and not clearly

distinguished in the spectra and therefore these features will not be further examined in the present studies. Nevertheless, it is noticed that for the spectra obtained for photon energies larger or equal to 91.7 eV, the Auger signal in the vicinity of the satellite peaks complicates the analysis of the data.

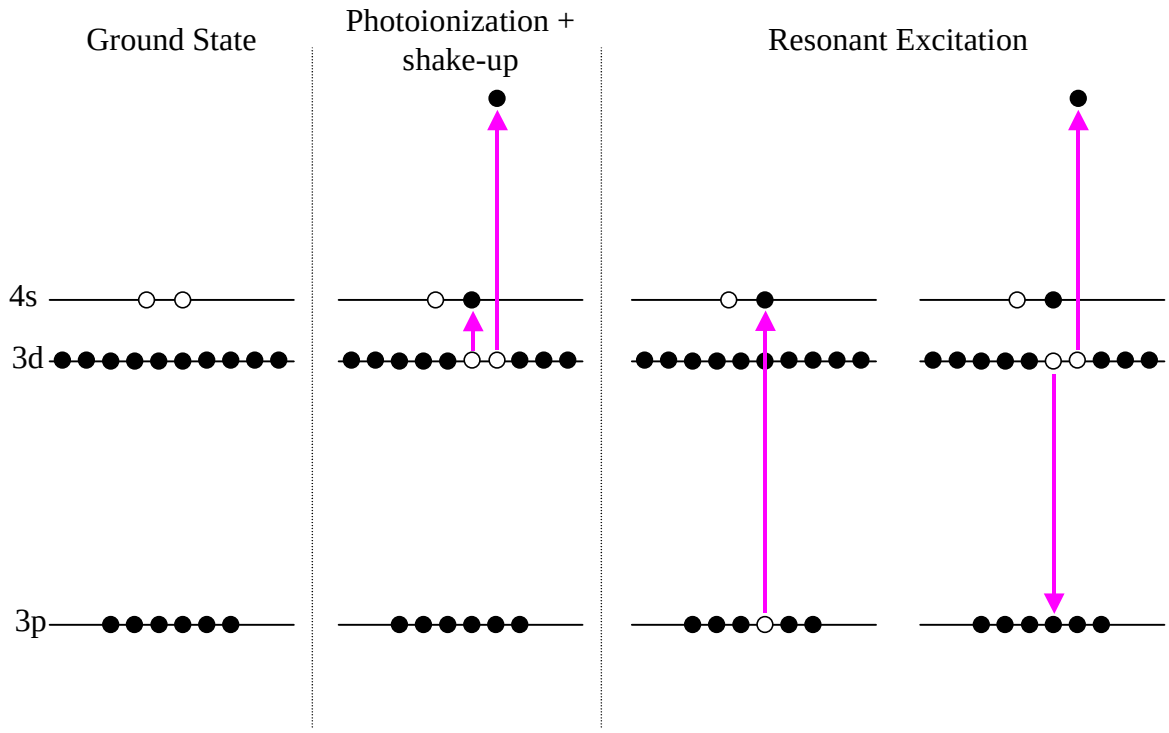

Fig. 6.4-4 Sketch of the ground state, of the final state reached after the 3d photoionization with shake-up, and of the final state reached after 3p-4s excitation for the Zn-porphyrazine compounds in the series. For simplification, the spin-orbit splitting of Zn3p level after 3p hole creation is neglected.

In order to get information about the satellite intensity dependence on the excitation energy, the satellite peaks region in the spectrum was fitted. The fit function was a sum of two Gaussians of equal widths, 1.07 eV, and constant separation of 3 eV between their centers (accounting for the satellite peaks) plus a linear function (in order to account for the background in that region). The widths of the satellite peaks and the separation between their centers were thus fixed parameters for the fit. Their values have been established from the analysis of the measured data at excitation energies where the satellite peaks are well observed but no Auger signal is detected. The method used for fitting the satellite region allows the estimation of the satellite areas.

For each photon energy, in order to determine the variation of the satellite peaks intensity as a function of the excitation energy, the obtained areas of the satellite peaks were divided by a normalization area taken in a pure background signal.

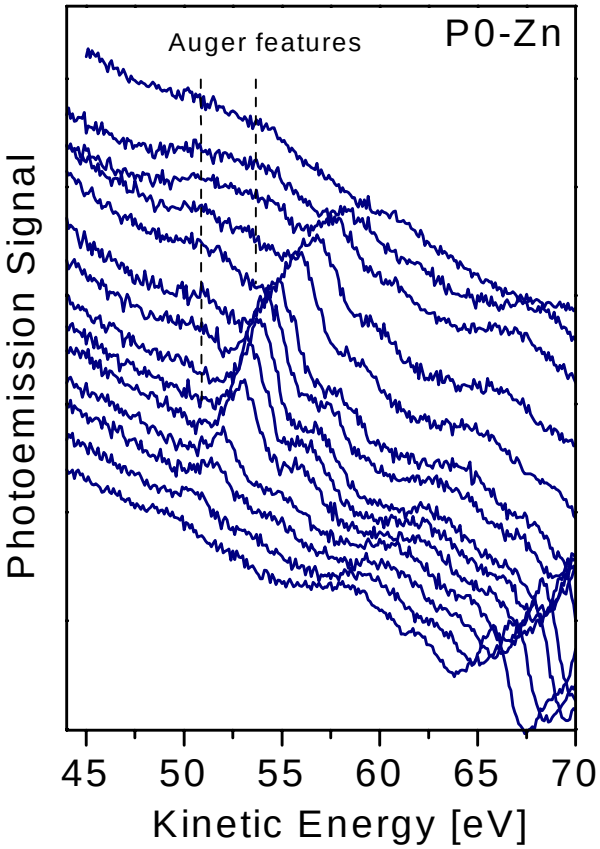

Fig. 6.4-5 Photoemission spectra of P0-Zn at (from bottom to top) 87.1, 88.1, 89.1, 89.6, 90.6, 91.1, 91.7, 92.2, 92.7, 93.7, 94.7, 95.7, 96.8, 98.7 eV photon energy. The Auger signal in the photoemission spectra is indicated.

By this procedure the influence of different synchrotron intensities on the photoemission signal was largely eliminated since the background signal is linearly dependent on the synchrotron light intensity. The relative area of the largest Zn satellite peak obtained in this way, for P0-Zn, P1-Zn and P2-Zn, is displayed in Fig. 6.4-6 for different excitation energies.

The systematic errors introduced by the fitting procedure have to be discussed. For small satellite intensities, the relative error in determining the areas becomes much larger than for the case when they are well distinguished. Generally, the fitting procedure overestimates the peak areas for small satellite intensities. This is the reason for having in Fig. 6.4-6 overestimated values of the satellite areas for off-resonant excitations where practically no satellite peak is observed by direct examining a spectrum of P0-Zn, P1-Zn or P2-Zn.

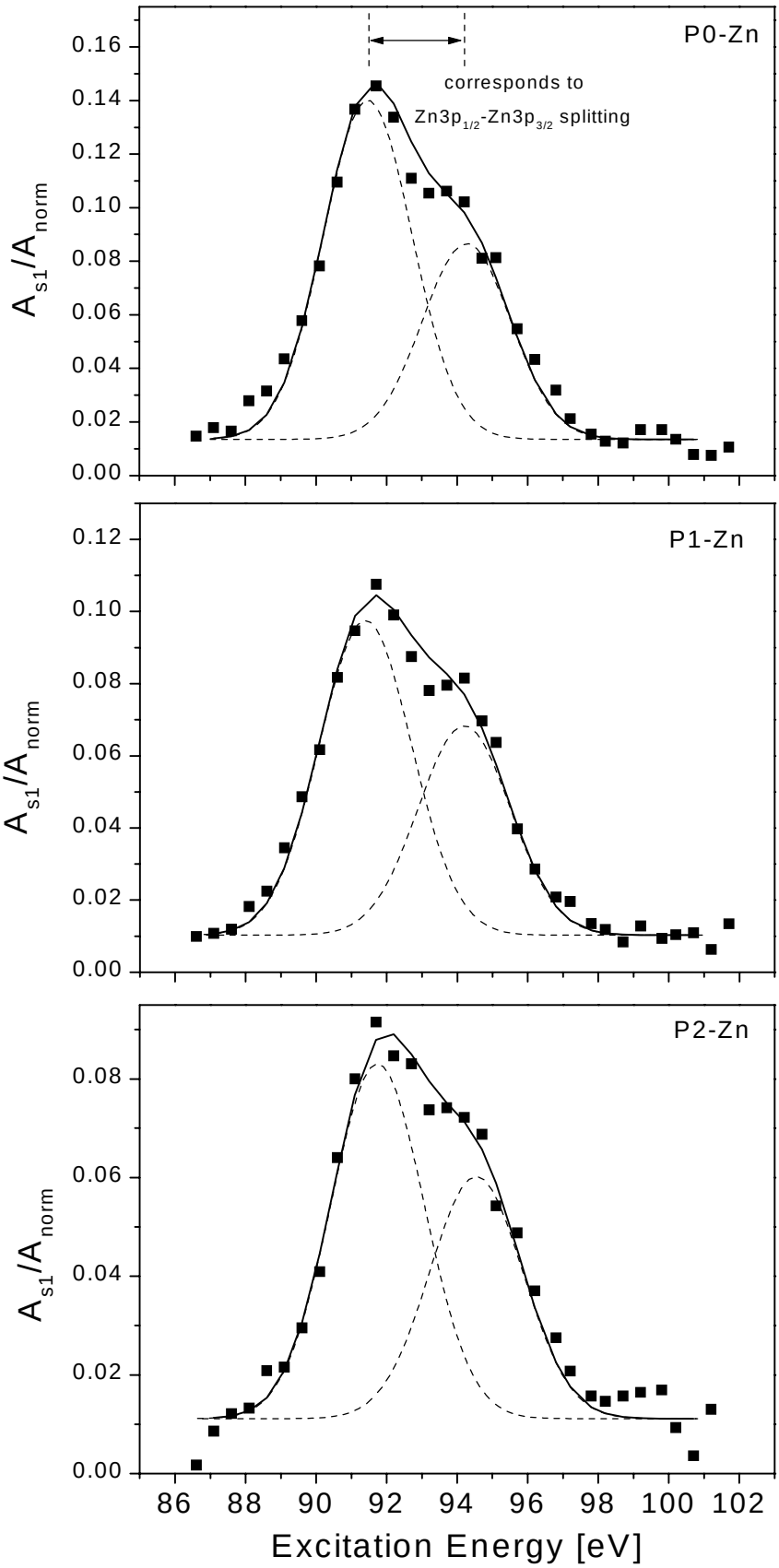

Fig. 6.4-6 The relative area of the largest Zn satellite peak as a function of the excitation energy for P0-Zn, P1-Zn and P2-Zn.

One can note that in Fig. 6.4-6, the relative area of the Zn satellite peak as a function of the excitation energy exhibits a double peak structure for all three Zn compounds. Similar behavior has been found for the sum area of both satellite peaks as a function of photon energy. The curve can be deconvoluted into a doublet with a splitting of ~2.8 eV, which we attribute to the excitation of the spin-orbit split components $3p_{1/2}$ and $3p_{3/2}$ of the Zn3p level. The presence of the two maxima indicates the involvement of both of the two possible final state configurations of the 3p hole in the process of 3p→4s electron excitation.

Therefore, the resonance curves were fit with a sum of two Gaussians of identical widths and with the separation between their centers equal to 2.8 eV (which corresponds to the $Zn3p_{1/2}$-$Zn3p_{3/2}$ splitting) plus a constant baseline. Ideally, this constant should be very close to zero, however, due to the systematic errors (previously mentioned) in determining the satellite areas, it appears with a larger value.

The resonance curve can be described by component peaks with similar widths and positions for the different compounds. The ratio between the area of the first peak component (corresponding to lower excitation energies on the axis) and the area of the second one appears to decrease at the extension of the ligand. However, this trend which can be seen in Fig. 6.4-6 is most likely introduced by broad and featureless Auger contributions for photon energies above the resonance, which modify the background there.

The manner the resonance curves in Fig. 6.4-6 were obtained doesn't allow a direct comparison of the satellite intensity for the different ligand extensions. This is due to the fact that the peak areas were normalized to areas taken in the background and the background signal differs significantly for P0-Zn, P1-Zn and P2-Zn.

In order to get information about the influence of the ligand extension on the satellite intensity, we compared the ratio between the satellite areas and the area of the Zn3d direct photoemission signal for the different molecules in the series.

To determine the area of the Zn3d contribution, the ligand signal has to be extracted from the spectrum. For that purpose, a background which had a Shirley and a linear component was first subtracted from both Zn- and corresponding metal-free compound spectra, as demonstrated in Fig. 6.4-7 and Fig. 6.4-8 for the cases of the P2-Zn and P2-H_2 spectra at 94.2 eV excitation energy. The combination of a linear plus Shirley-type background was accounting in a satisfactory way for the shape of the background.

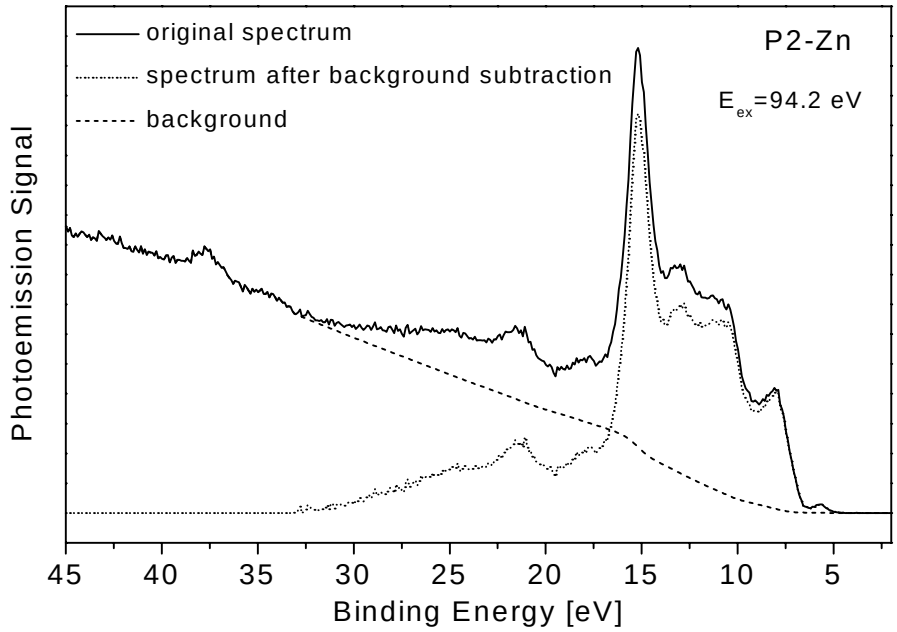

Fig. 6.4-7 The original spectrum, the calculated background, and the spectrum after background subtraction for P2-Zn at 94.2 eV excitation energy.

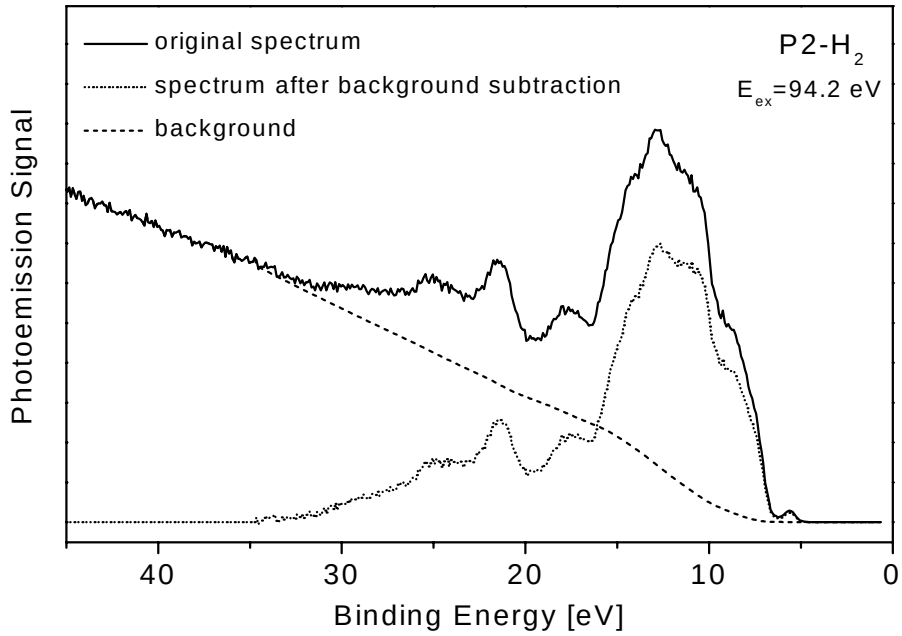

Fig. 6.4-8 The original spectrum, the calculated background, and the spectrum after background subtraction for P2-H_2 at 94.2 eV excitation energy.

In a next step, for obtaining the area of the Zn3d direct photoemission signal, each metal-free compound spectrum (after background subtraction) was overlapped at the ligand features with the corresponding zinc compound spectrum (also background-subtracted). Subsequently, the difference spectrum was integrated at the position of Zn3d main line. Identical integration ranges were assured for all compounds at all excitation energies.

In order to exemplify the manner of determining the area of the Zn3d direct photoemission signal, Fig. 6.4-9 presents the overlapped P2-Zn and P2-H_2 spectra (both after background subtraction) and the difference spectrum obtained for 94.2 eV.

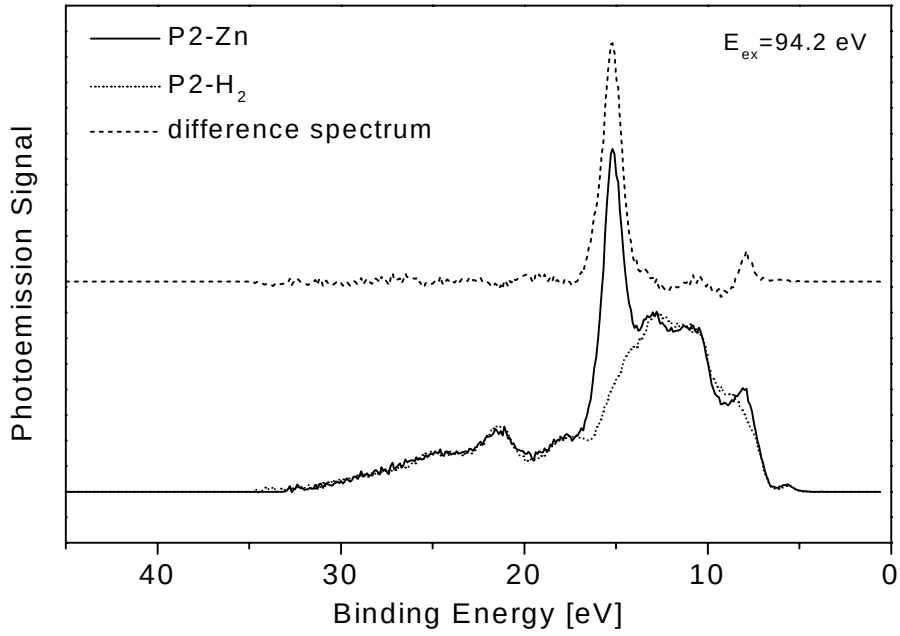

Fig. 6.4-9 The overlapped background-subtracted P2-Zn and P2-H_2 spectra. The dashed curve represents the difference between the background-subtracted P2-Zn and P2-H_2 spectra.

The ratios between the area of the Zn satellite peaks and the area of the Zn3d main line as a function of excitation energy for P0-Zn, P1-Zn and P2-Zn are displayed in Fig. 6.4-10. The top panel of Fig. 6.4-10 depicts the ratio between the area of the larger satellite peak (A_{s1}) and the area of the Zn3d main line (AZn_{3d}) while the lower panel shows the ratio between the sum area of both satellite peaks ($A_{s1}+A_{s2}$) and the area of Zn3d main line. In the figure the error bars are shown only for P2-Zn in several points but for each of the graphs the error bars are identical for all three compounds, in all points (but their value in the top graph differs from the one in the bottom graph).

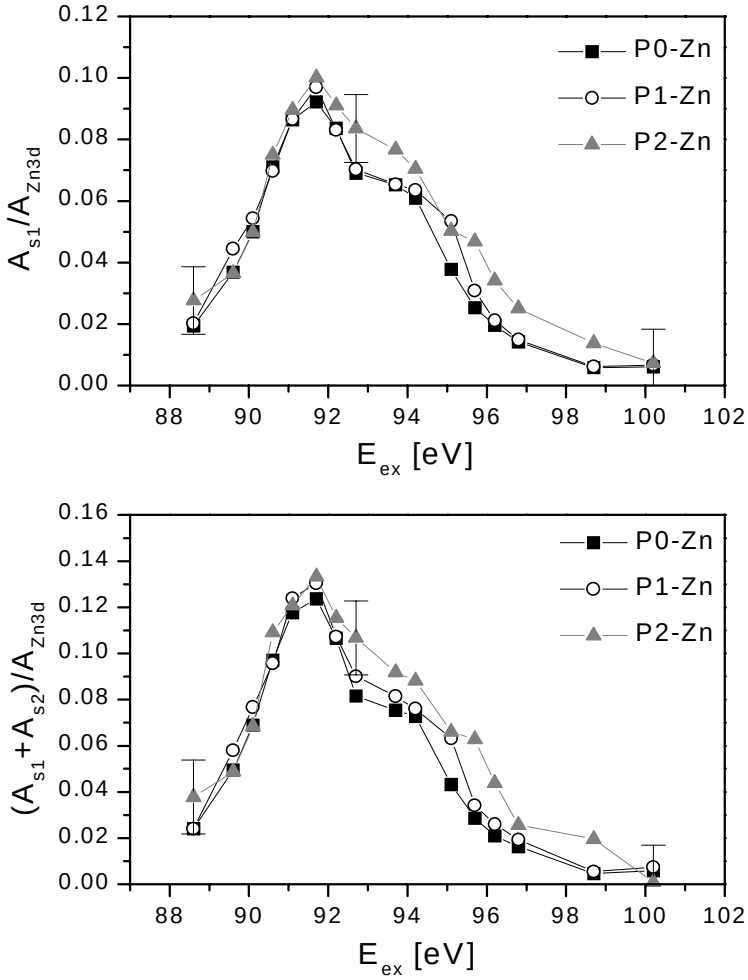

Fig. 6.4-10 Comparison of the ratios between the area of the Zn satellite peaks and the area of Zn3d main line as a function of the excitation energy for P0-Zn, P1-Zn and P2-Zn. The top panel displays the ratio between the area of the larger satellite peak, centered at ~37.8 eV binding energy, and the area of Zn3d main line. The lower panel shows the ratio between the sum area of both satellite peaks and the area of the Zn3d main line. For each graph the error bars are identical for all three compounds, in all points.

Since there is a dependence of the cross section of the Zn3d signal on the excitation energy, in comparing these ratios for ZnPc and P1-Zn and in general for all Zn molecules in the series, one should utilize only the points obtained for the same photon energy.

One can notice in Fig. 6.4-10 that up to 91.7 eV excitation energy the intensity ratios appear nearly identical for P0-Zn, P1-Zn and P2-Zn, while for higher photon energies larger values are obtained for P2-Zn than for the other two compounds. This behavior appears consistent with the dependence seen in the resonance curves (a decrease of the ratio between the first and the second component of the resonance curve for P2-Zn). This indicates that the different values of satellite to main line intensity ratios for P2-Zn arise from the calculated satellite areas in the fitting procedure and not from the determined

Zn3d areas. Thus, the differences in the satellite/main line intensity ratios for photon energies larger than 91.7 eV, which exist for P0-Zn, P1-Zn, and P2-Zn, are caused by an incorrect area estimation for the satellite peaks in the fitting procedure. The factors responsible for this discrepancy are the Auger signal in the vicinity of the satellite peaks, in combination with the differences in the background shape in the spectra of those compounds.

Therefore, we conclude that the satellite/main line intensity ratios in the present measurements are within the error bars identical for P0-Zn, P1-Zn and P2-Zn. This would suggest the existence of the same number of free 4s states for all three compounds, and consequently the same degree of covalent (or ionic) character of the bond between Zn and ligand.

Similar to the case of metal-free compounds, the inner porphyrazine ring and consequently the distance between the opposite pyrrole nitrogen atoms and between zinc and pyrrole nitrogen, increase at linear benzoannelation. Theoretical calculations estimated an increase of the Zn-N distance from 1.979 Å in ZnTAP to ~1.981 Å in ZnPc [NgP2001]. To the best of our knowledge, no experimental determination of the Zn-N distance has been reported up to date for ZnTAP. However, theoretical and experimental works established that the metal-nitrogen distance in ZnPc is larger than in CuPc. In Ref. [LiS2001] it was calculated that the Cu-N_p (N_p=pyrrole nitrogen) distance in CuPc is 1.976 Å while the Zn-N_p distance in ZnPc is 2.012 Å. Recent experiments determined that the Cu-N_p distance in CuPc is 1.935 Å [MRF2000] and the Zn-N_p one in ZnPc is 1.954 Å [RMF99].

The present experimental results support the following argumentation. Presumably in P0-Zn, P1-Zn, and P2-Zn, the metal-pyrrole nitrogen distance being larger than for the corresponding copper compounds, it increases by a smaller amount with linear benzoannelation than for the copper porphyrazines. On the other side, in the present experiments, by determining the effect of the 3p-4s resonant excitation we are not sufficiently sensitive for evidencing very small changes. These facts would explain to our opinion that, even if the Zn-N_p distance increases for the zinc compounds with linear benzoannelation, and consequently differences in the covalent character of the metal-ligand bond could exist, the changes are too small to be detected here.

6.5 P3-Zn Compound

The P3-Zn compound deserves extra consideration because a P3-Zn film could not be obtained by UHV sublimation. Therefore, films of P1-Zn and P3-Zn have been prepared by the wet chemical method described in Chapter 3. The situation is analogous to that for the copper complexes.

Despite the use of the same wet chemical method for preparing these films as for the ones obtained for P2-Cu and P3-Cu, the P1-Zn and P3-Zn films turned out to be unstable. After measurements the films were dissolved and their optical absorption spectra were determined. Those revealed significant differences as compared to the absorption spectra of the original materials, indicating that part of the materials has been transformed (probably into radical cations). The respective photoemission spectra for P1-Zn and P3-Zn films obtained by wet chemical method at 91.7 eV photon energy are presented in Fig. 6.5-1. For comparison also the photoemission spectrum at the same photon energy of an UHV sublimed P1-Zn film is added.

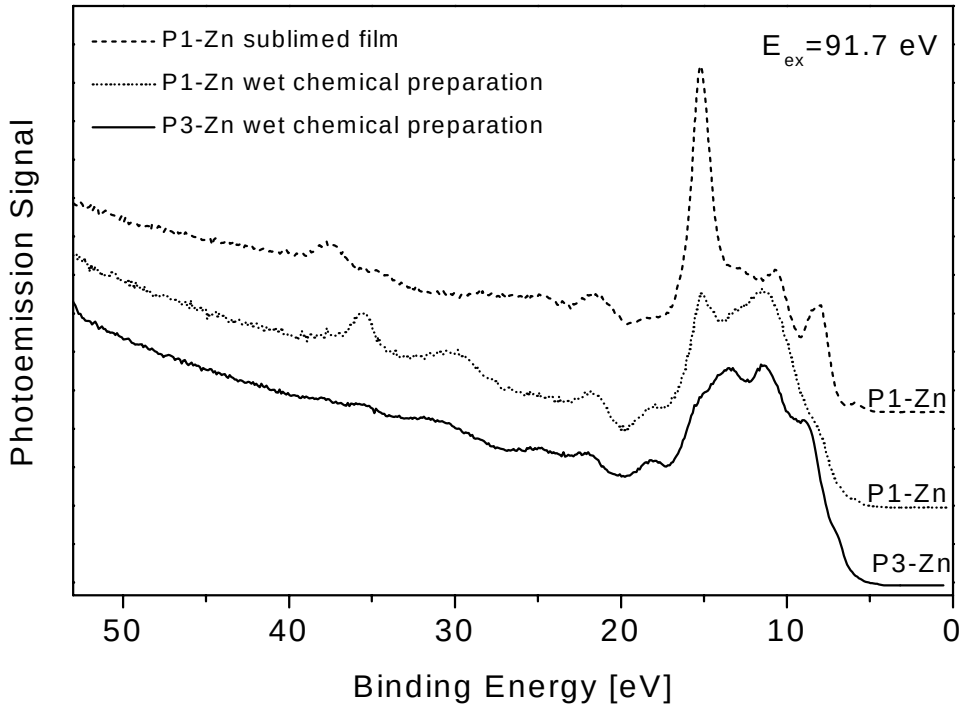

Fig. 6.5-1 Photoemission spectra of P1-Zn and P3-Zn films, prepared by wet chemical method, along with the corresponding spectra obtained for a UHV sublimed P1-Zn film.

The binding energy scale for the P1-Zn wet chemically obtained film was established by aligning the main Zn3d peak with the corresponding one of the UHV sublimed film. For P3-Zn the energy scale was established by aligning its ligand peaks with those of the P1-Zn wet chemically prepared film.

By comparing the three curves in Fig. 6.5-1 one notices a much poorer quality of the spectra obtained for the ex-situ prepared films. Actually, this was the first indication that the compounds might be degraded. The intensity of the Zn3d main peak relative to the ligand features is much lower in comparison with the case of sublimed films. Thus, for P3-Zn the Zn3d direct photoemission signal is not resolved anymore, being embedded in a dominant, most probably, ligand-derived signal.

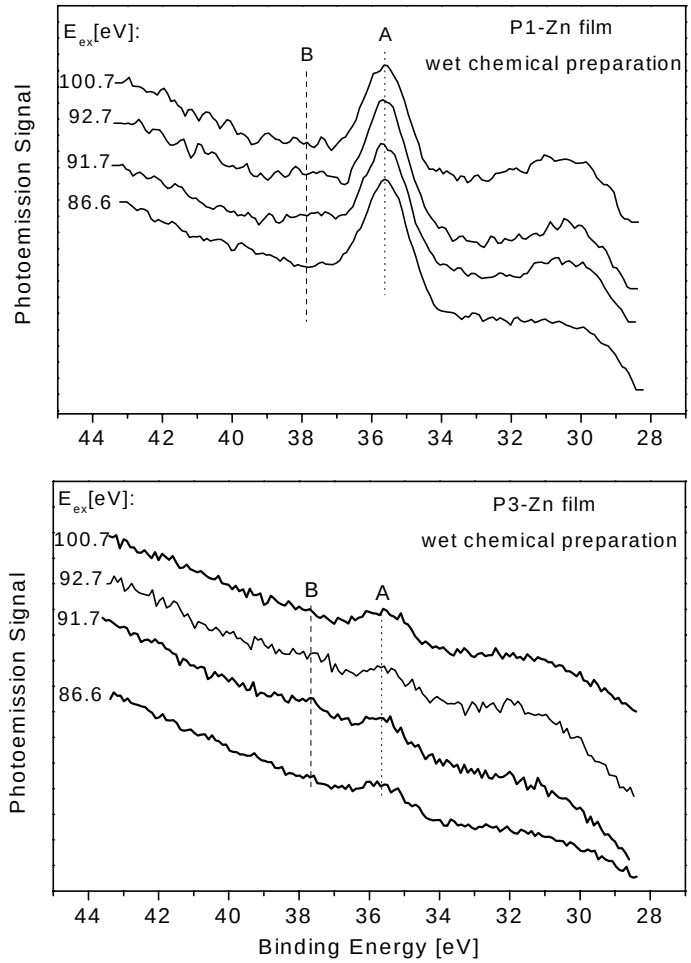

Fig. 6.5-2 Photoemission spectra in the region of Zn satellite peaks from P1-Zn (top) and P3-Zn (bottom) at several photon energies. Both films have been deposited ex-situ, using a wet chemical method. Peak B represents most probably satellite signal but peak A doesn't originate from satellite signal.

Since parts of the films were still containing the intact compound, the satellite peaks region has been investigated in more detail. The spectra in the region of Zn satellites obtained from the wet chemically prepared P1-Zn and P3-Zn films, for several photon energies, are presented in Fig. 6.5-2.

In the spectra obtained from the P1-Zn film, we observe a fairly intense peak, denoted by A, whose intensity is not influenced by the excitation energy. As this peak is observed for energies at which the Zn satellite peaks are not visible, it clearly indicates that this is not a satellite peak. In addition to peak A, in the spectra at 91.7 and 92.7 eV of P1-Zn film, one notices a small feature (denoted B), on the high binding energy side of peak A. For 86.6 and 100.7 eV this feature B appears to be absent. Its binding energy, ~37.85 eV, is roughly the same as for the larger Zn satellite peak in the spectrum of P1-Zn film deposited by UHV sublimation. This and the fact that peak B appears to exist in the spectrum only at energies for which the Zn satellite peaks are also visible, indicates that feature B might arise from the Zn satellite signal of intact molecules.

A similar situation occurs in the measurements of P3-Zn film deposited by the wet chemical method. A clear peak (denoted A in Fig. 6.5-2 bottom) appears at 35.6 eV binding energy, independent of photon energy. For the same reasons as previously discussed for the peak A in the spectrum of wet chemical prepared P1-Zn film, this feature for P3-Zn is concluded to not represent Zn satellite signal. In the spectra obtained for 91.7 and 92.7 eV excitation energy, a weak feature, denoted B, is found at roughly 37.7 eV binding energy. Thus, its position is close to the one of the larger satellite peak in the spectra of UHV deposited Zn compounds. Similarly to the case of identically prepared P1-Zn film, this feature is not observed for 86.6 and 100.7 eV photon energies. Consequently, feature B might be associated with a Zn satellite signal originating from the P3-Zn molecules which were left intact within the film.

Of course, considering the poor quality of the ex-situ prepared P1-Zn and P3-Zn films, it is difficult to draw clear conclusion on the basis of these experiments. Nevertheless, the behavior observed in the spectra could probably indicate that a P3-Zn film, containing only intact molecules, may exhibit Zn satellite peaks showing a similar behavior as for the other zinc compounds in the series.

6.6 Summary

This chapter presents the photoemission experiments performed on a set of compounds containing zinc as central metal atom, namely ZnPc, P0-Zn, P1-Zn, and P2-Zn. The study of the spectra of the valence region shows a decrease in the HOMO binding energy with stepwise linear benzoannelation, which is similar to that observed for the metal-free porphyrazines series. XPS measurements showed no changes larger than the experimental accuracy limits in the separation between C1s and N1s or C1s and Zn2p peaks with the extension of the ligand. Zinc satellite peaks are clearly visible in the spectra of the valence region for 3p-4s resonant excitation. The intensity ratios between these satellite peaks and the Zn3d main line have similar values for P0-Zn, P1-Zn, and P2-Zn below 91.7 eV excitation energy. Differences in the covalent character of the bond between zinc and ligand for those compounds are thus not reflected in the present measurements by changes in the satellite to main line intensity ratios. We suggest the following two main reasons for the observed behavior. First, the central C_8N_8 ring in these molecules is larger than in the corresponding copper compounds and therefore we propose that it increases by a smaller amount with linear benzoannelation than for the copper porphyrazines. Thus, expected differences in the covalent character of the bond between the central metal and the ligand are smaller for the compounds in the zinc series than for those in the copper series. Secondly, the experimental procedure used to infer these differences in covalency is not sufficiently sensitive for evidencing such small changes.